Psychological Medicine (2016), **46**, 1225–1238. © Cambridge University Press 2016
doi:10.1017/S0033291715002767

ORIGINAL ARTICLE

Different neural substrates for executive functions in youths with ADHD: a diffusion spectrum imaging tractography study

H.-L. Chiang[1,2,3], Y.-J. Chen[4], C.-Y. Shang[1], W.-Y. I. Tseng[4,5,6]* and S. S.-F. Gau[1,2,5]*

[1] *Department of Psychiatry, National Taiwan University Hospital and College of Medicine, Taipei, Taiwan*
[2] *Graduate Institute of Clinical Medicine, College of Medicine, National Taiwan University, Taipei, Taiwan*
[3] *Department of Psychiatry, Far Eastern Memorial Hospital, New Taipei City, Taiwan*
[4] *Institute of Medical Device and Imaging, National Taiwan University College of Medicine, Taipei, Taiwan*
[5] *Graduate Institute of Brain and Mind Sciences, National Taiwan University College of Medicine, Taipei, Taiwan*
[6] *Department of Medical Imaging, National Taiwan University Hospital, Taipei, Taiwan*

Background. The relationship between white-matter tracts and executive functions (EF) in attention deficit hyperactivity disorder (ADHD) has not been well studied and previous studies mainly focused on frontostriatal (FS) tracts. The authors explored the microstructural property of several fibre tracts hypothesized to be involved in EF, to correlate their microstructural property with EF, and to explore whether such associations differ between ADHD and typically developing (TD) youths.

Method. We assessed 45 youths with ADHD and 45 individually matched TD youths with a computerized test battery for multiple dimensions of EF. From magnetic resonance imaging, FS tract, superior longitudinal fasciculus (SLF), arcuate fasciculus (AF) and cingulum bundle (CB) were reconstructed by diffusion spectrum imaging tractography. The generalized fractional anisotropy (GFA) values of white-matter tracts were computed to present microstructural property of each tract.

Results. We found lower GFA in the left FS tract, left SLF, left AF and right CB, and poorer performance in set-shifting, sustained attention, cognitive inhibition and visuospatial planning in ADHD than TD. The ADHD and TD groups demonstrated different association patterns between EF and fibre tract microstructural property. Most of the EF were associated with microstructural integrity of the FS tract and CB in TD youths, while with that of the FS tract, SLF and AF in youths with ADHD.

Conclusions. Our findings support that the SLF, AF and CB also involve in a wide range of EF and that the main fibre tracts involved in EF are different in youths with ADHD.

Received 30 May 2015; Revised 12 November 2015; Accepted 16 November 2015; First published online 8 January 2016

Key words: Attention deficit hyperactivity disorder, diffusion spectrum imaging, executive function, tractography.

Introduction

Executive functions (EF) have been suggested to be cognitive endophenotypes for ADHD, which are closely linked to underlying pathogenesis of ADHD (Bidwell *et al.* 2007; Gau & Shang, 2010*a*). With the advances of brain-imaging technique, functional and structural changes in the brain have been recognized as a primary cause underlying the behavioural problems of attention deficit hyperactivity disorder (ADHD; Liston *et al.* 2011). Functional imaging studies have shown that youths with ADHD had less frontostriatal (FS) activation during performance of executive tasks (Konrad *et al.* 2006), and that adults with ADHD engaged different brain areas during the performance of cognitive tasks (Dibbets *et al.* 2010). In previous structural (Tamm *et al.* 2012; Shang *et al.* 2013) and functional (Hart *et al.* 2013) neuroimaging studies of ADHD, the importance of FS circuitry on executive control has been most consistently reported. In fact, a meta-analysis study suggested that alterations in white-matter integrity were widespread in patients with ADHD (van Ewijk *et al.* 2012), and recent studies also highlighted the alteration of other fibre tracts in youths with ADHD, such as superior longitudinal fasciculus (SLF; Pavuluri *et al.* 2009; Lawrence *et al.* 2013) and cingulum bundle (CB; Pavuluri *et al.* 2009), but their relationship with EF are still undetermined.

* Address for correspondence: S. S.-F. Gau, M.D., Ph.D., Department of Psychiatry, National Taiwan University Hospital and College of Medicine, No. 7, Chung-Shan South Road, Taipei 10002, Taiwan.

(Email: gaushufe@ntu.edu.tw) [S.S.-F.G]
(Email: wytseng@ntu.edu.tw) [W.-Y.I.T]

Until now, there has been only one study investigating the association between white-matter tract and EF in ADHD (Shang *et al.* 2013), demonstrating different association patterns between EF and the microstructural property of FS tracts in youths with ADHD. Since SLF (Ge *et al.* 2013), arcuate fasciculus (AF; Kucukboyaci *et al.* 2012; Lebel *et al.* 2013) and CB (Kantarci *et al.* 2011; Lebel *et al.* 2013; Ikuta *et al.* 2014) have been recognized to be associated with EF in healthy participants (Kucukboyaci *et al.* 2012; Ge *et al.* 2013), older adults (Kantarci *et al.* 2011) and individuals with other neuropsychiatric conditions (Lebel *et al.* 2013; Ikuta *et al.* 2014), we intend to include these fibre tracts, as well as FS tracts, into analysis in the current study.

Using a matched case-control study design at the individual level, we compared the white-matter microstructural property and analysed its relationship with EF. Additionally, we analysed white-matter tracts with diffusion spectrum imaging (DSI), one of the high angular resolution diffusion imaging techniques, to address the limitation of diffusion tensor imaging (DTI) to resolve the crossing fibres (Wedeen *et al.* 2008). Unlike the principal direction of the DTI that points to a direction somewhere between the crossing fibres, DSI provides an advantageous method whereby the directions of the maxima of the average propagator correspond to the underlying crossing fibre directions (Lin *et al.* 2003). We hypothesized that the microstructural property of these white-matter tracts might differ in youths with ADHD from typically developing (TD) youths. Furthermore, we also investigated whether the diffusion anisotropy of these target tracts correlated with EF, and whether there were altered association patterns in youths with ADHD compared to TD youths.

Method

Participants and procedures

The Research Ethics Committee of National Taiwan University Hospital approved this study prior to its implementation (approved number 200903062R, ClinicalTrials.gov number NCT00916851). Both participants and their parents provided written informed consent. All participants received clinical evaluation and their parents received psychiatric interviews with the Chinese version of the Schedule for Affective Disorders and Schizophrenia for School-Age Children – Epidemiologic Version (K-SADS-E; Gau *et al.* 2005) about the diagnosis of the participants. All the participants were tested with the Wechsler Intelligence Scale for Children – 3rd edition (WISC-III) and the Cambridge Neuropsychological Test Automated Battery (CANTAB).

Youths with ADHD were recruited consecutively at the Department of Psychiatry, National Taiwan University Hospital. They were clinically diagnosed with ADHD according to the DSM-IV-TR diagnostic criteria, and confirmed by the psychiatric interviews with the Chinese version of the K-SADS-E. The TD youths, referred by the school principals and teachers, were recruited from the same school districts as the ADHD group. They and their parents also received the Chinese K-SADS-E interview to confirm that they did not have lifetime or current ADHD diagnosis and other psychiatric disorders. Exclusion criteria for all the participants include psychosis, mood disorders, learning disability, substance use disorder, autism spectrum disorder, neurological disorders, current diagnosis of anxiety disorders, or a full-scale IQ score <80. Of the eligible 53 pairs of youths with ADHD and individually sex-, age-, handedness-, IQ-, and coil-matched TD youths, eight ADHD patient-control pairs were excluded due to the suboptimal quality of the imaging data. A total of 45 ADHD patients and 45 controls remained in the final analysis (Table 1, detailed information about DSI quality assurance is provided in the Supplementary Material). Among the 45 youths with ADHD, 22 (49%) were of the combined type, 22 (49%) were of the predominantly inattentive type, and one (2%) was of the predominantly hyperactivity/impulsivity type. Ten of them had been treated with methylphenidate before or currently, and treatment of methylphenidate was discontinued at least 1 week before neuropsychological and magnetic resonance imaging (MRI) assessment.

A subset of the sample (10 of 45 ADHD youths, 20 of 45 TD youths) was included in a previously published work using a different DSI analysis method (Shang *et al.* 2013). However, the study hypotheses of this study are different from those in Shang *et al.* (2013). Shang *et al.* (2013) only focused on the FS tracts, while the current study focused on the association between EF and the microstructural property of other major fibre tracts (i.e. SLF, AF, CB) based on different DSI method (Large Deformation Diffeomorphic Metric Mapping, LDDMM), under the consideration of the effect of FS tracts on other target fibre tracts.

Clinical measures

Chinese version of the K-SADS-E

The K-SADS-E is a semi-structured interview scale for the systematic assessment of both lifetime and current diagnosis of mental disorders in children and adolescents. The preparation of the Chinese K-SADS-E includes a two-stage translation and modification of several items with psycholinguistic equivalents relevant to the Taiwanese culture and further modification

Table 1. *Demographics, IQ, ADHD subtype, ADHD symptoms of children with ADHD and typically developing children*

	ADHD ($n = 45$)	TD ($n = 45$)	t values	p values
Gender, male (%)	33 (73.3 %)	33 (73.3 %)		
Handedness: right *v.* left	44 *v.* 1	44 *v.* 1		
Coil: 32 *v.* 16	42 *v.* 3	42 *v.* 3		
Age (mean±S.D.) (range 7–18 yr)	11.36 ± 2.86	11.29 ± 2.71	0.62	0.538
Full-scale IQ (mean±S.D.)	109.98 ± 11.6	111.42 ± 11.21	−0.8	0.43
Performance IQ	108.93 ± 13.44	108 ± 13.29	0.40	0.692
Verbal IQ	109.49 ± 10.75	113.31 ± 9.78	−2.63	0.012
DSM-IV symptom count[a] (mean±S.D.)				
Inattention (0–9)	7.64 ± 1.36	0.33 ± 0.9	30.17	<0.001
Hyperactivity (0–6)	2.99 ± 1.93	0.16 ± 0.46	9.67	<0.001
Impulsivity (0–3)	1.62 ± 1.11	0 ± 0	9.82	<0.001

S.D., Standard deviation; IQ, intelligence quotient; ADHD, attention deficit hyperactivity disorder; TD, typically developing children.

[a] Based on psychiatric interview using the Kiddie-SADS-E interviews of the current symptoms.

Table 2. *Correlations between fibre tract microstructural property and ADHD symptoms in youths with ADHD*

	Inattention		Hyperactivity/impulsivity	
Correlations (p value)	Left	Right	Left	Right
Striatum-VLPFC	−0.35 (0.02)	−0.33 (0.028)	−0.14 (0.361)	−0.06 (0.692)
Striatum-DLPFC	−0.29 (0.051)	−0.34 (0.022)	0.03 (0.841)	0.05 (0.748)
Striatum-OFC	−0.28 (0.061)	−0.31 (0.041)	−0.04 (0.780)	0.01 (0.969)
Superior longitudinal fasciculus	−0.42 (0.004)	−0.51 (<0.001)	0.19 (0.222)	0.07 (0.663)
Arcuate fasciculus	−0.38 (0.010)	−0.47 (0.001)	0.35 (0.017)	0.20 (0.179)
Cingulum bundle	−0.46 (0.002)	−0.47 (0.001)	0.01 (0.954)	0.08 (0.624)

ADHD, Attention deficit hyperactivity disorder; TD, typically developing children; VLPFC, ventrolateral prefrontal cortex; DLPFC, dorsolateral prefrontal cortex; OFC, orbitofrontal cortex.

to meet DSM-IV diagnostic criteria (Gau *et al.* 2005). The Chinese K-SADS-E is a reliable and valid instrument to assess DSM-IV child and adolescent psychiatric disorders, and has been widely used in a variety of studies regarding childhood mental disorders [e.g. clinic-based research (Gau & Shang, 2010*a*; Gau *et al.* 2010, *2014*; Shang *et al.* 2011; Tseng & Gau, 2013; Gau & Huang, 2014), and clinical trials (Gau & Shang, 2010*b*; Ni *et al.* 2013)] to make the psychiatric diagnoses in child and adolescent populations in Taiwan.

Chinese version of the Swanson, Nolan, and Pelham, version IV scale (SNAP-IV) – Parent Form

The Chinese SNAP-IV is a 26-item rating scale with nine items for inattention symptoms, nine items for hyperactivity/impulsivity symptoms and eight items for oppositional symptoms according to DSM-IV symptom criteria of ADHD and oppositional defiant disorder (ODD). Items are rated as a 4-point Likert scale (0, not at all; 1, just a little; 2, quite a lot; 3, very much). The norm and psychometric properties of the Chinese SNAP-IV – Parent Form have been established (Gau *et al.* 2008). The Chinese SNAP-IV has been widely used in assessing ADHD and ODD symptoms in clinical and research settings in Taiwan (e.g. Shang *et al.* 2013; Yang *et al.* 2013; Chien *et al.* 2014). We used the symptom-count criterion from the full diagnostic criteria of DSM-IV to demonstrate the severity of ADHD symptoms in this study.

EF measures

The CANTAB is a computerized test battery which has been validated and widely used worldwide (Gau *et al.* 2009; Chamberlain *et al.* 2011). It is designed to be administered by trained psychologists with standardized procedures. Five tasks of the CANTAB involving EF were administered to all the participants in this study (Gau & Shang, 2010*a*; Shang *et al.* 2013).

Intra-extra dimensional set shift (IED)

The IED, a computerized analogue of the Wisconsin Card Sorting test, is used to assess an individual's ability to selectively maintain attention on the specific attribute of compound stimuli across different examples, or intra-dimensional shift (e.g. colour-filled shapes remain the only relevant dimension), and then to shift their attention to a previously irrelevant attribute of stimuli, or extra-dimensional shift (white lines become the only relevant dimension) (Downes *et al.* 1989). After six correct consecutive responses, the computer changes the sorting rules. Two major indices were included in the present study: (1) adjusted total errors: calculated by adding 25 for each stage not attempted due to failure; and (2) adjusted total trials: adding 50 for each stage not attempted due to failure at an earlier stage.

Rapid visual information processing (RVP)

The RVP, a 4-min visual continuous performance test, is designed to assess sustained attention. Digits, from 2 to 9 in a random order, appear one at a time at a rate of 100 digits per minute in the centre of the screen. The participant has to detect three target sequences (2–4–6, 3–5–7, 4–6–8) and respond when the last number is seen (6, 7, 8, respectively). The participant was instructed to detect as many target sequences (27 in total) as possible. Three indices were presented in the present study: (1) probability of false alarms (the participant responding inappropriately): total false alarms divided by the sum of total false alarms and total correct rejections; (2) B'': a signal detection measure of the strength of trace required to elicit a response and lower score indicates higher response tendency; and (3) mean latency: mean time taken to respond in correct responses.

Spatial span

This task measures spatial short-term memory and is the visuospatial analogue of the digit span test. Nine white boxes were presented in fixed locations on the screen. The colour of the boxes changed one after the other in a predetermined sequence. Participants were required to remember the order of the boxes in which the colour was changed, and to point to the boxes on the screen in the order as previously presented by the computer. The task begins at the 2-box level then gradually maximally increases to the 9-box level. There are three sequences at each level. If the participant fails in all three sequences at a particular level the test will terminate. Two indices were used in the present study: (1) span length: the longest sequence successfully recalled; and (2) total usage errors: the number of times a box was selected that was not in the sequence being recalled.

Spatial working memory (SWM)

This task assesses non-verbal working memory based on a self-ordered search test (Luciana & Nelson, 1998). Participants were asked to search through a number of coloured boxes presented on the screen to find a blue token hidden inside. The participants had to memorize the boxes which had been opened in each trial and the boxes in which the tokens had been found in the previous trial. Two indices were used in this study: (1) total errors: total times the participant visits a box that is sure not to have a blue token, i.e. either a token inside in previous trial or empty in this trial; and (2) strategy utilization: the number of search sequences starting with a novel box to assess the ability of participants to adopt a sequential search pattern, so that a higher score indicated poorer use of strategy.

Stocking of Cambridge (SOC)

The SOC task assesses spatial planning based on the Tower of London test (Luciana & Nelson, 1998), and requires the participants to move balls according to a goal position with given orders and locations. Three suspended vertical stockings and three coloured balls were presented on the monitor screen, and participants were required to move the coloured balls to accomplish a goal position within a specified number of moves. Three major indices are presented in this article: (1) problems solved in the specified minimum number of moves: the number of occasions which were successfully completed in the minimum possible number of moves; (2) total moves: the total number of moves taken in excess of the specified minimum moves but within the maximum allowed; and (3) initial thinking time: the difference in reaction time taken to select the first ball for the same problem under the two conditions.

MRI data acquisition

MRI data were acquired on a 3-T MRI machine (Trio, Siemens, Germany) with a 32-channel phased-array head coil except three dyads with a 16-channel phased-array head coil (Table 1). A sagittal localizer was used to define a line between the anterior commissure and posterior commissure, which was then used to define imaging planes orthogonal to it. T1-weighted images covering the whole head were acquired using a 3D magnetization-prepared rapid gradient echo (MPRAGE) sequence, repetition time (TR) = 2530 ms; echo time (TE) = 3.4 ms; slice thickness = 1.0 mm; matrix size = 256 × 192 × 208; and field of view (FOV) = 256 × 192 × 208 mm^3. Transaxial DSI data were acquired using a pulsed-gradient spin-echo EPI sequence with a twice-refocused balanced echo (Reese *et al.* 2003). An acquisition scheme which comprised 102 diffusion-weighted image (DWI) volumes (101 diffusion gradient vectors + 1 null image) corresponding to the grid points within a half sphere of the *q*-space (DSI 102) were applied with the maximum diffusion sensitivity value ($b_{\max}$) set to 4000 s/mm^2 (Kuo *et al.* 2008). Other acquisition parameters were TR = 9600 ms; TE = 130 ms; matrix size = 80 × 80; FOV = 200 × 200 mm^2; slice number = 56 and slice thickness = 2.5 mm without gap. The scan time for DSI acquisition was approximately 16.5 min.

DSI reconstruction

The acquired DSI data allowed us to reconstruct the diffusion probability density function (PDF) based on the Fourier relationship between the PDF and *q*-space signal. Within each voxel, there were 102 samples at the grid points within a half sphere of the *q*-space. These 102 samples were projected around the origin to fill the other half sphere based on the fact that the *q*-space data were symmetric around the origin. The eight corners outside the sphere were filled with zeros, resulting in a 7 × 7 × 7 data grid in the *q*-space. A Hanning filter of 17 units in width was applied to the *q*-space data, followed by a 3D Fourier transform of the *q*-space signal to obtain the PDF. The orientation distribution function [ODF, $\psi(u)$] was computed by obtaining the second moment of the PDF along each of the 362 radial directions (6-fold tessellated icosahedron). At each voxel, generalized fractional anisotropy (GFA) was quantified in terms of s.d.(ψ)/RMS(ψ), where s.d. is the standard deviation and RMS is the root mean square. The GFA indicates the directionality of the ODF and ranges from zero (when diffusion is completely random in three dimensions) to one (when diffusion is extremely restricted to one dimension only) (Tuch, 2004). To determine the local tract directions in each voxel, an iterative approach was used to decompose the ODF into several constituent Gaussian ODFs (Yeh *et al.* 2011). The resulting local tract direction field was obtained for tractography.

Tract-specific analysis

To avoid subjective variation arising from manual tractography, a template-based approach was employed. The procedures are illustrated in Supplementary Fig. S1. A study-specific DSI template was constructed from all the recruited participants using a nonlinear registration method under the framework of LDDMM (Hsu *et al.* 2012). A streamline-based algorithm adapted for DSI data (Yeh *et al.* 2013) was performed on the study-specific DSI template, and 12 target tract bundles were reconstructed using expert-monitored multiple regions of interest (ROIs) approach (Lo *et al.* 2011) based on Automatic Anatomical Labeling (AAL) system (Tzourio-Mazoyer *et al.* 2002). Having segmented each target tract bundle on the study-specific DSI template, the coordinates of streamlines were aligned along the proceeding direction of each tract bundle and were saved as the sampling coordinates. The sampling coordinates of target tracts were then transformed from the study-specific DSI template to individual DSI dataset according to the established transformation between the study-specific DSI template and the individual DSI dataset in native space. Consequently, the GFA values of each target tract were sampled on the corresponding sampling coordinates in native space.

The target tracts included bilateral FS tracts, i.e. striatum-ventral lateral prefrontal cortex (VLPFC), striatum-dorsal lateral prefrontal cortex (DLPFC), and striatum-orbital frontal cortex (OFC), SLF (the combination of SLF I, SLF II, and SLF III), CB, and AF (Fig. 1). For the FS tracts, ROIs were placed at the striatum (putamen + caudate) and the prefrontal cortical regions. The VLPFC was defined as the combination of the inferior frontal gyrus and middle frontal gyrus. The DLPFC was defined as the combination of the medial frontal gyrus and superior frontal gyrus. The OFC was defined as the combination of the middle orbitofrontal gyrus, superior orbitofrontal gyrus, medial orbitofrontal gyrus, and inferior orbitofrontal gyrus. For the SLF, the ROIs were placed at the superior frontal gyrus and precuneus (SLF I), at the triangular part of the inferior frontal gyrus and middle occipital gyrus (SLF II), and at the opercular part of the inferior frontal gyrus and angular gyrus (SLF III). For the CB, the ROIs were placed at the anterior, middle, and posterior parts of the cingulate gyrus. For the AF, the ROIs were placed at the opercular part of the inferior frontal gyrus and superior temporal gyrus. The coordinates of these ROIs in AAL were transformed to the study-specific DSI template via the transformation between the study-specific DSI template and the ICBM 152 template using a 'Dartel' toolbox in SPM 12 (Ashburner & Friston, 2011). Streamlines that passed through the selected ROIs simultaneously were segmented as a tract bundle. DSI tractography was performed using DSI Studio (http://dsi-studio.labsolver.org). Tract bundles were verified to ensure the consistency with the established anatomical landmarks (Wakana *et al.* 2005).

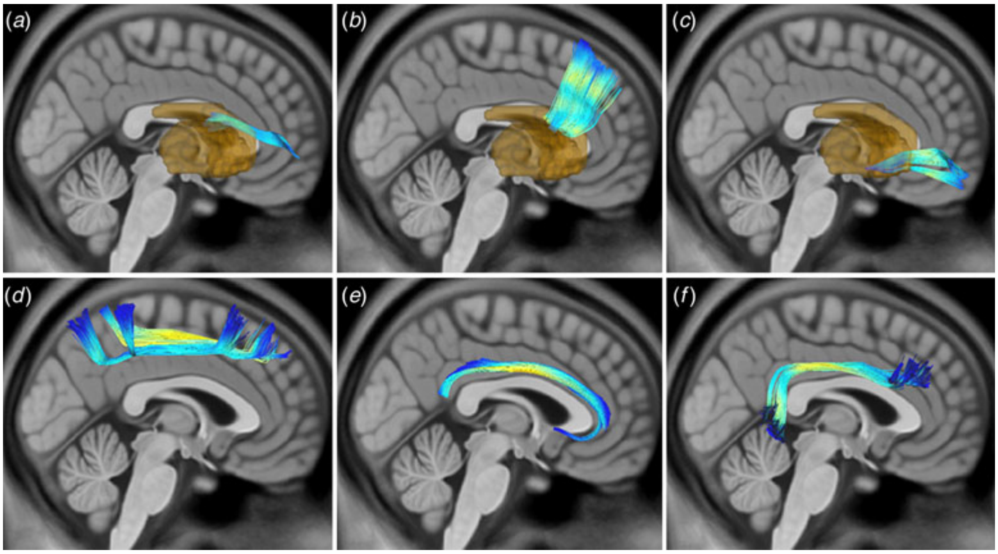

Fig. 1. Reconstruction of the targeted tracts in the right hemisphere. (*a*) Striatum-ventrolateral prefrontal tract; (*b*) striatum-dorsolateral prefrontal tract; (*c*) striatum-orbitofrontal tract; (*d*) superior longitudinal fasciculus I, II and III; (*e*) cingulum bundle; (*f*) arcuate fasciculus. The regions of interest at the striatum (brown) are shown in (*a*)–(*c*).

Statistical analyses

Data analysis was conducted using SAS version 9.2 (SAS Institute Inc., USA). The alpha value was preselected at the level of $p < 0.05$. The descriptive results are displayed as the mean and S.D. for the continuous variables. Because of the matched case-control study design, we used paired *t* test to compare the mean scores of IQ, ADHD symptom counts, the CANTAB performance, and the GFA values of the white-matter tracts between the ADHD and TD groups. Cohen's *d* was computed to indicate small (d=0.2–0.5), medium (d=0.5–0.8), and large (d>0.8) effect sizes.

To control for the inflation of Type I error in computing multiple bivariate correlations, multiple linear regression models with the backward elimination procedure were conducted to determine the relationship between the indexes of EF and the GFA values of the 12 fibre tracts: bilateral FS tracts, including striatum-VLPFC, striatum-DLPFC, and striatum-OFC, SLF, AF and CB, as independent variables. The GFA values of the 12 targeted tracts were entered as independent variables, and each of the index on the CANTAB tasks, as the dependent variables. We used backward elimination procedure to identify the fitted model containing the variables from these 12 tracts which maintained significant effects on each of the measures. The R^2 values were calculated to present the proportion of the variance of each measure that can be explained by the microstructural property, presented by the GFA values, of some of the fibre tracts in the final fitted model. Because we wanted to investigate disease-specific patterns between white-matter tracts and EF in youths with ADHD, which was hypothesized to be different from the patterns in TD youths, we conducted the above-mentioned multivariate regression analyses stratifying by the ADHD and TD groups. We also tested the interactions between group and mean GFA value of tracts on the indexes of EF to decide whether the magnitude of the associations between tract GFA values and EF varied between the two groups.

Results

Demographics

As expected, we found no significant group differences in the distribution of gender, handedness, age, full-scale IQ, performance IQ, and the type of coil used during MRI assessment between youths with ADHD and TD youths. Youths with ADHD had lower verbal IQ than TD youths (Table 1).

Microstructural property

Compared to TD youths, youths with ADHD had significantly lower mean GFA values in all three left FS tracts (i.e. striatum-VLPFC, striatum-DLPFC, striatum-OFC), left SLF, left AF and right CB (Fig. 2 and Supplementary Table S1) with small effect sizes (Cohen's d=0.35–0.5).

EF

Youths with ADHD tended to perform worse than TD youths in some indexes of the CANTAB tasks

https://doi.org/10.1017/S0033291715002767 Published online by Cambridge University Press

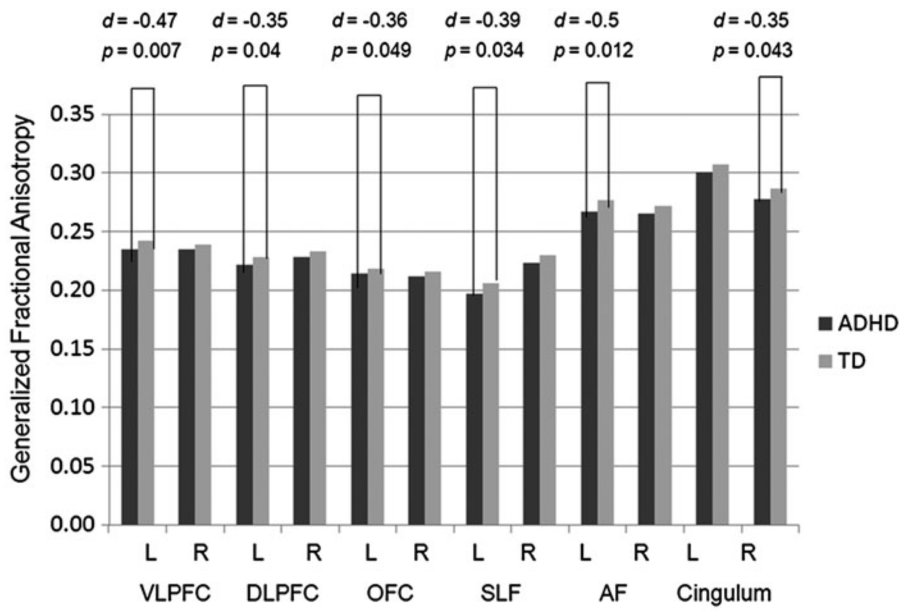

Fig. 2. Comparisons of the mean generalized fractional anisotropy for bilateral striatum-dorsolateral (DLPFC), striatum-ventrolateral (VLPFC), striatum-orbitofrontal (OFC), superior longitudinal fasciculus (SLF); arcuate fasciculus (AF) between youths with attention deficit hyperactivity disorder (ADHD) and typically developing (TD) youths. L, Left; R, right; *d*, Cohen's *d*.

involving EF with medium to large effect sizes (Cohen's d=0.47–0.81) (Supplementary Table S2). Compared to TD youths, youths with ADHD had significantly more total errors and total trials to complete the tasks in IED, had lower response tendency as indexed by RVP B'' value, and fewer problems solved in minimum moves, more total moves needed and shorter mean initial thinking time in SOC.

Correlations of fibre tract property with ADHD symptoms

Using the ADHD symptoms assessed by SNAP-IV, the GFA values of bilateral striatum-VLPFC tracts, right striatum-DLPFC tract, right striatum-OFC tract, bilateral SLF, AF and CB were negatively correlated with inattention symptoms in youths with ADHD ($p <$ 0.05, Table 2). Instead, the GFA values of these targeted tracts did not correlate with hyperactivity/impulsivity symptoms, except for positive association with the left AF.

Correlations of fibre tract property with performance of EF

Association patterns of the microstructural property of fibre tracts, indicated by the GFA values, with indexes of EF in the final fitted model were presented separately in TD youths (Table 3) and in youths with ADHD (Table 4). In addition to FS tracts, CB was associated with most of the EF (i.e. sustained attention, working memory and planning) in TD youths, while SLF and AF were associated with most of the EF (i.e. sustained attention, short-term memory, working memory and planning) in youths with ADHD. Additionally, the left striatum-OFC tract and left CB were not correlated with any EF in youths with ADHD.

Specifically, the striatum-VLPFC tract property was significantly associated with performance of spatial sustained attention (RVP), working memory (SWM) and planning (SOC) in TD youths, while with set-shifting (IED), short-term memory (spatial span) and planning (SOC) in youths with ADHD. The striatum-DLPFC tract property was significantly associated with the performance of sustained attention, short-term memory and planning in TD youths as well as in youths with ADHD. The striatum-OFC tract property was significantly associated with the performance of working memory and planning in TD youths, while with sustained attention, working memory and planning in youths with ADHD. The SLF tract property was significantly associated with the performance of sustained attention and planning in TD youths, while with sustained attention, short-term memory, working memory and planning in youths with ADHD. The AF tract property was significantly associated with the performance of sustained attention in TD youths, while with sustained attention, short-term memory, working memory and planning in youths with ADHD. The CB tract property was significantly associated with the performance of sustained attention,

https://doi.org/10.1017/S0033291715002767 Published online by Cambridge University Press

Table 3. *Final models of the link between white-matter tracts and executive functions in typically developing children*

	Rapid visual information processing			Spatial span	Spatial working memory		Stockings of Cambridge		
β (p value)	Probability of false alarm	B'' (response tendency)	Mean latency, ms	Total usage errors	Total errors	Strategy utilization	Problems solved in minimum moves	Total moves	Mean initial thinking time, ms
Striatum-VLPFC									
Left								−61.77 (0.042)	
Right	−0.592 (0.014)	2.33 (0.063)				−249.58 (0.011)			
Striatum-DLPFC									
Left								−51.07 (0.073)	
Right	0.456 (0.086)			−23.68 (0.04)					
Striatum-OFC									
Left								90.85 (0.088)	
Right						270.09 (0.015)			
SLF									
Left			−2577.36 (0.079)				−59.78 (0.003)	19.07 (0.099)	−48 198 (0.01)
Right							52.69 (0.01)		
Arcuate fasciculus									
Left	−0.517 (0.054)	4.33 (0.018)							
Right	0.553 (0.023)	−2.99 (0.002)	3728.52 (0.025)						
Cingulum									
Left	−0.358 (0.011)	2.05 (0.037)							33 181 (0.063)
Right			−3537.18 (0.025)		−314.79 (0.003)	−80.49 (0.074)			
F value (p value)	$F_{5,39} = 5.63$ (<0.001)	$F_{4,40} = 5.37$ (0.002)	$F_{3,41} = 3.22$ (0.033)	$F_{1,43} = 4.47$ (0.040)	$F_{1,43} = 9.67$ (0.003)	$F_{3,41} = 4.69$ (0.007)	$F_{2,42} = 5.19$ (0.01)	$F_{4,40} = 2.91$ (0.033)	$F_{2,42} = 3.67$ (0.034)
R^2	0.42	0.35	0.19	0.09	0.18	0.26	0.20	0.23	0.15

β, Estimate of regression coefficient; RT, reaction time; S.E., standard errors; ISI, inter-stimulus intervals; VLPFC, ventrolateral prefrontal cortex; DLPFC, dorsolateral prefrontal cortex; OFC, orbitofrontal cortex; SLF, superior longitudinal fasciculus.

Table 4. *Final models of the link between white-matter tracts and executive functions in children with ADHD*

	Intra-extra dimensional set shift		Rapid visual information processing		Spatial span		Spatial working memory		Stockings of Cambridge		
β (*p* values)	Total errors, adjusted	Total trials, adjusted	B'' (response tendency)	Mean latency, ms	Span length	Total usage errors	Total errors	Strategy utilization	Problems solved in minimum moves	Total moves	Mean initial thinking time, ms
Striatum-VLPFC											
Left											75 768 (0.008)
Right	−696.94 (0.004)	−1242.23 (0.003)				−60.47 (0.005)					
Striatum-DLPFC											
Left						38.79 (0.066)					−45 378 (0.081)
Right				−5277.09 (0.011)							
Striatum-OFC											
Right				5723.41 (0.087)			−377.94 (0.049)		89.65 (<0.001)	−84.93 (<0.001)	
SLF											
Left					−63.73 (0.003)			−109.47 (0.002)	−52.04 (0.023)		
Right			8.22 (0.028)	−6665.49 (<0.001)	82.728 (<0.001)	−43.09 (0.01)	−473.09 (0.008)		41.45 (0.044)		
Arcuate fasciculus											
Left				7098.72 (<0.001)		36.66 (0.044)	325.87 (0.072)				−40 545 (0.095)
Right			−6.2 (0.076)								53 883 (0.012)
Cingulum											
Right											−38 361 (0.012)
F values (*p* values)	$F_{1,43} = 9.51$ (0.004)	$F_{1,43} = 9.9$ (0.003)	$F_{2,42} = 2.63$ (0.084)	$F_{4,40} = 10.76$ (<0.001)	$F_{2,42} = 11.57$ (<0.001)	$F_{4,40} = 6.98$ (<0.001)	$F_{3,41} = 9.91$ (<0.001)	$F_{1,43} = 10.65$ (0.002)	$F_{3,41} = 12.21$ (<0.001)	$F_{1,43} = 19.16$ (<0.001)	$F_{5,39} = 4.27$ (0.003)
R^2	0.18	0.19	0.11	0.52	0.36	0.41	0.42	0.20	0.47	0.31	0.35

ADHD, Attention deficit hyperactivity disorder; β, estimate of regression coefficient; RT, reaction time; s.e., standard errors; ISI, inter-stimulus intervals; VLPFC, ventrolateral prefrontal cortex; DLPFC, dorsolateral prefrontal cortex; OFC, orbitofrontal cortex; SLF, superior longitudinal fasciculus.

short-term memory, working memory and planning in the TD youths, while only with planning in youths with ADHD.

Interactions between the diagnostic group (ADHD v. TD) and fibre tract microstructural properties on the indexes of EF

We further test the interactions between group and mean GFA value of tracts on the indexes of EF. Statistical significance of interaction terms are noted in several tracts in terms of different indexes, including the left striatum-VLPFC tract with sustained attention ($p = 0.009$) and short-term memory ($p = 0.047$); the right striatum-VLPFC tract with set shitting ($p = 0.028$ in total errors; $p = 0.021$ in total trials); the right striatum-DLPFC tract with and sustained attention ($p = 0.042$) and planning ($p = 0.033$ in problems solved in minimum moves; $p = 0.022$ in total moves); the left striatum-OFC tract with sustained attention ($p = 0.008$) and planning ($p = 0.028$ in problems solved in minimum moves; $p = 0.019$ in total moves); the right striatum-OFC tract with working memory ($p = 0.017$) and planning ($p < 0.001$ in problems solved in minimum moves; $p = 0.002$ in total moves); the right SLF with sustained attention ($p = 0.02$), short-term memory ($p = 0.005$ in span length; $p = 0.044$ in total usage errors) and working memory ($p = 0.003$); the left SLF with working memory ($p = 0.038$) and planning ($p = 0.037$); and the right CB with working memory ($p = 0.011$) and planning ($p = 0.045$) (Supplementary Table S3).

Discussion

We conducted a strictly individually matched case-control diffusion imaging study with the strengths of comprehensive investigation of several major fibre tracts hypothesized to be involved with EF, use of the state-of-the-art DSI tractography analysis, and assessment of multiple dimensions of EF in a relatively larger sample than previous investigation. This study demonstrated that youths with ADHD had lower GFA in the left FS tracts, left SLF, left AF and right CB, and presented probably different association patterns of fibre tract microstructural property and EF between youths with ADHD and TD youths.

FS tracts and EF

Early studies investigating white-matter property in ADHD mainly focused on FS tracts, but most of them did not report the difference in the left and right sides (Pavuluri *et al.* 2009; de Zeeuw *et al.* 2012). Our finding of significantly decreased GFA in only the left FS tracts in ADHD youths is supported by the collateral evidence that youths with ADHD had reduced white-matter volume specific to the left hemisphere (Mostofsky *et al.* 2002).

Our findings that FS tracts property is associated with EF in both ADHD and TD youths are consistent with some of previous studies (Shang *et al.* 2013). Our findings of the association of EF with FS tracts connecting the bilateral striatum-VLPFC, -DLPFC and -OFC tracts in both groups except no association of the left striatum-OFC tract with EF in youths with ADHD suggest that altered striatum-OFC tract by demonstrating the loss of the association between its microstructural property and EF in youths with ADHD might contribute to observed impaired EF among youths with ADHD.

SLF and EF

Our finding of decreased GFA of the left SLF in youths with ADHD is consistent with previous studies (Hamilton *et al.* 2008; Pavuluri *et al.* 2009; Lawrence *et al.* 2013; King *et al.* 2015), but inconsistent with Lawrence *et al.* reporting only difference in mean diffusivity, rather than fractional anisotropy (Lawrence *et al.* 2013). Besides, our study design is unique because we investigated the association between EF and other white-matter tracts under consideration of the effect of the FS tracts. We found that the SLF tract property is associated with sustained attention, short-term memory, working memory and planning in the ADHD group, but only with sustained attention and planning in the TD group. Our results are consistent with others reporting the association between working memory and the structural connectivity of the left (Vestergaard *et al.* 2011) and bilateral (Peters *et al.* 2012) SLF in TD youths.

AF and EF

To the best of our knowledge, this is the first study to report decreased diffusion anisotropy of AF in ADHD. Previous studies have reported associations of AF with the performance of set-shifting test (Kucukboyaci *et al.* 2012) and visual attention (Lebel *et al.* 2013) in healthy controls. Since problems in attention and set-shifting are frequently reported in ADHD (Shang *et al.* 2013; Wu *et al.* 2014), it is not surprising that AF was one of the altered white-matter tracts of ADHD in the current study.

Although the AF is well known to be responsible for language function, recent studies demonstrated that the AF is a long segment of the SLF connecting the temporal lobe with the lateral frontal cortex, a broader region than the Broca's area (Martino *et al.* 2013). Therefore, the current study provides evidence to support that the AF may involve in the networks of cognitive functions other than language in TD youths and youths with ADHD as well. We also demonstrate that the microstructure property of AF was associated with most of the EF (except the performance of set-shifting) in ADHD youths, but only with the performance of the sustained attention in TD youths. Because youths with ADHD had lower verbal IQ than TD youths in the current study, we also examined the correlation between the GFA values of the AF and verbal IQ, and found no correlation in both groups.

CB and EF

Our finding of decreased diffusion anisotropy in the right CB is consistent with some studies of adults with childhood ADHD (Makris *et al.* 2008) and youths with ADHD (Silk *et al.* 2009; Peterson *et al.* 2011), but is not supported by other studies in youths with ADHD (Hamilton *et al.* 2008; Lin *et al.* 2014). With a larger sample size, our findings may provide more convincing evidence. The CB has been reported to be associated with sustained attention (Takahashi *et al.* 2010) and EF (Peters *et al.* 2014) in healthy subjects, and with intra-individual variability in reaction time in youths with ADHD (Lin *et al.* 2014). Unlike the microstructure property of the SLF and AF, which are associated with more domains of EF in ADHD youths, the CB seems to better explain the performance of EF in TD youths in the current study. The different association patterns lend evidence to support the hypothesis that ADHD may engage adaptive processing strategies to compensate for impairments in EF (Coghill *et al.* 2014) and also in other brain regions (Fassbender & Schweitzer, 2006). That is, some EF depending on the CB in TD youths might get compensation from the SLF and AF in youths with ADHD.

Methodological consideration

Our study has some limitations. First, whether the different diffusion anisotropy of white-matter tracts in youths with ADHD reflects the underlying neuropathology of ADHD or the consequences of a compensatory neurodevelopment process cannot be determined in this cross-sectional study. Second, long-term effects of medication on microstructural property may exist in ten youths with ADHD who ever treated with methylphenidate in this study, although no significant differences in fractional anisotropy between medicated and drug-naive children with ADHD has been reported in a recent DTI study (de Luis-Garcia *et al.* 2015). We also try to minimize the influence of medication that all of our medicated youths had discontinued methylphenidate at least 1 week before neuropsychological and MRI assessment. Third, due to the low percentage of hyperactive-impulsive type in the ADHD group, our results may be more applicable to youths with ADHD, combined type and those with inattentive type. Fourth, due to restricting the sample to a more homogenous group by inclusion and exclusion criteria, generalization of the findings to other populations is questionable. Lastly, due to the scarce literature on this topic, we presented original statistical results to allow readers to evaluate the importance and significance of the results without adjusting for multiple comparisons (Veazie, 2006).

Conclusion

This study provides strong evidence that the SLF, AF and CB also involve in the core neuropathological underpinnings of ADHD. Additionally, differential association patterns between youths with ADHD and TD youths imply the possible compensatory mechanism. Studies to examine other fibre tracts theoretically associated with ADHD neuropathology, to collect longitudinal data to shed light on the developmental trajectories of different diffusion anisotropy of white-matter tracts in ADHD are warranted.

Supplementary material

For supplementary material accompanying this paper visit http://dx.doi.org/10.1017/S0033291715002767

Acknowledgements

This work was supported by grants from the National Science Council (NSC99-2627-B-002-015, NSC100-2627-B-002-014, NSC101-2627-B-002-002, NSC101-2321-B-002-079), National Taiwan University Hospital (NTUH101-S1910), and Ministry of Economic Affairs (101-EC-17-A-19-S1-175), Taiwan. The manuscript preparation was supported by National Health Research Institute (NHRI-EX102-10008PI), Taiwan. (ClinicalTrials.gov number: NCT01677793, NCT 00916851.)

Declaration of Interest

None.

References

Ashburner J, Friston KJ (2011). Diffeomorphic registration using geodesic shooting and Gauss-Newton optimisation. *Neuroimage* **55**, 954–967.

Bidwell LC, Willcutt EG, Defries JC, Pennington BF (2007). Testing for neuropsychological endophenotypes in siblings discordant for attention-deficit/hyperactivity disorder. *Biological Psychiatry* **62**, 991–998.

Chamberlain SR, Robbins TW, Winder-Rhodes S, Muller U, Sahakian BJ, Blackwell AD, Barnett JH (2011). Translational approaches to frontostriatal dysfunction in attention-deficit/hyperactivity disorder using a computerized neuropsychological battery. *Biological Psychiatry* **69**, 1192–1203.

Chien YL, Gau SS, Chiu YN, Tsai WC, Shang CY, Wu YY (2014). Impaired sustained attention, focused attention, and vigilance in youths with autistic disorder and Asperger's disorder. *Research in Autism Spectrum Disorders* **8**, 881–889.

Coghill DR, Hayward D, Rhodes SM, Grimmer C, Matthews K (2014). A longitudinal examination of neuropsychological and clinical functioning in boys with attention deficit hyperactivity disorder (ADHD): improvements in executive functioning do not explain clinical improvement. *Psychological Medicine* **44**, 1087–1099.

de Luis-Garcia R, Cabus-Pinol G, Imaz-Roncero C, Argibay-Quinones D, Barrio-Arranz G, Aja-Fernandez S, Alberola-Lopez C (2015). Attention deficit/hyperactivity disorder and medication with stimulants in young children: a DTI study. *Progress in Neuro-Psychopharmacology and Biological Psychiatry* **57**, 176–184.

de Zeeuw P, Mandl RC, Hulshoff Pol HE, van Engeland H, Durston S (2012). Decreased frontostriatal microstructural organization in attention deficit/hyperactivity disorder. *Human Brain Mapping* **33**, 1941–1951.

Dibbets P, Evers EA, Hurks PP, Bakker K, Jolles J (2010). Differential brain activation patterns in adult attention-deficit hyperactivity disorder (ADHD) associated with task switching. *Neuropsychology* **24**, 413–423.

Downes JJ, Roberts AC, Sahakian BJ, Evenden JL, Morris RG, Robbins TW (1989). Impaired extra-dimensional shift performance in medicated and unmedicated Parkinson's disease: evidence for a specific attentional dysfunction. *Neuropsychologia* **27**, 1329–1343.

Fassbender C, Schweitzer JB (2006). Is there evidence for neural compensation in attention deficit hyperactivity disorder? A review of the functional neuroimaging literature. *Clinical Psychology Review* **26**, 445–465.

Gau SS, Chiu CD, Shang CY, Cheng AT, Soong WT (2009). Executive function in adolescence among children with attention-deficit/hyperactivity disorder in Taiwan. *Journal of Developmental and Behavioral Pediatrics* **30**, 525–534.

Gau SS, Chong MY, Chen TH, Cheng AT (2005). A 3-year panel study of mental disorders among adolescents in Taiwan. *American Journal of Psychiatry* **162**, 1344–1350.

Gau SS, Huang WL (2014). Rapid visual information processing as a cognitive endophenotype of attention deficit hyperactivity disorder. *Psychological Medicine* **44**, 435–446.

Gau SS, Lin YJ, Cheng AT, Chiu YN, Tsai WC, Soong WT (2010). Psychopathology and symptom remission at adolescence among children with attention-deficit-hyperactivity disorder. *Australian & New Zealand Journal of Psychiatry* **44**, 323–332.

Gau SS, Shang CY (2010*a*). Executive functions as endophenotypes in ADHD: evidence from the Cambridge Neuropsychological Test Battery (CANTAB). *Journal of Child Psychology and Psychiatry* **51**, 838–849.

Gau SS, Shang CY (2010*b*). Improvement of executive functions in boys with attention deficit hyperactivity disorder: an open-label follow-up study with once-daily atomoxetine. *International Journal of Neuropsychopharmacology* **13**, 243–256.

Gau SS, Shang CY, Liu SK, Lin CH, Swanson JM, Liu YC, Tu CL (2008). Psychometric properties of the Chinese version of the Swanson, Nolan, and Pelham, version IV scale – parent form. *International Journal of Methods in Psychiatric Research* **17**, 35–44.

Gau SS, Tseng WL, Tseng WY, Wu HY (2014). Association between microstructural integrity of frontostriatal tracts and school functioning: ADHD symptoms and executive function as mediators. *Psychological Medicine* **30**, 1–15.

Ge H, Yin X, Xu J, Tang Y, Han Y, Xu W, Pang Z, Meng H, Liu S (2013). Fiber pathways of attention subnetworks revealed with tract-based spatial statistics (TBSS) and probabilistic tractography. *PLoS ONE* **8**, e78831.

Hamilton LS, Levitt JG, O'Neill J, Alger JR, Luders E, Phillips OR, Caplan R, Toga AW, McCracken J, Narr KL (2008). Reduced white matter integrity in attention-deficit hyperactivity disorder. *Neuroreport* **19**, 1705–1708.

Hart H, Radua J, Nakao T, Mataix-Cols D, Rubia K (2013). Meta-analysis of functional magnetic resonance imaging studies of inhibition and attention in attention-deficit/hyperactivity disorder: exploring task-specific, stimulant medication, and age effects. *JAMA Psychiatry* **70**, 185–198.

Hsu YC, Hsu CH, Tseng WY (2012). A large deformation diffeomorphic metric mapping solution for diffusion spectrum imaging datasets. *Neuroimage* **63**, 818–834.

Ikuta T, Shafritz KM, Bregman J, Peters BD, Gruner P, Malhotra AK, Szeszko PR (2014). Abnormal cingulum bundle development in autism: a probabilistic tractography study. *Psychiatry Research* **221**, 63–68.

Kantarci K, Senjem ML, Avula R, Zhang B, Samikoglu AR, Weigand SD, Przybelski SA, Edmonson HA, Vemuri P, Knopman DS, Boeve BF, Ivnik RJ, Smith GE, Petersen RC, Jack CR Jr. (2011). Diffusion tensor imaging and cognitive function in older adults with no dementia. *Neurology* **77**, 26–34.

King JB, Yurgelun-Todd D, Stoeckel A, DiMuzio JM, Lopez-Larson MP (2015). Sex differences in white matter integrity in youths with attention-deficit/hyperactivity disorder: a pilot study. *Frontiers in Neuroscience* **9**, 232.

Konrad K, Neufang S, Hanisch C, Fink GR, Herpertz-Dahlmann B (2006). Dysfunctional attentional networks in children with attention deficit/hyperactivity disorder: evidence from an event-related functional magnetic resonance imaging study. *Biological Psychiatry* **59**, 643–651.

Kucukboyaci NE, Girard HM, Hagler DJ Jr., Kuperman J, Tecoma ES, Iragui VJ, Halgren E, McDonald CR (2012). Role of frontotemporal fiber tract integrity in task-switching performance of healthy controls and patients with temporal lobe epilepsy. *Journal of the International Neuropsychological Society* **18**, 57–67.

Kuo LW, Chen JH, Wedeen VJ, Tseng WY (2008). Optimization of diffusion spectrum imaging and q-ball imaging on clinical MRI system. *Neuroimage* **41**, 7–18.

Lawrence KE, Levitt JG, Loo SK, Ly R, Yee V, O'Neill J, Alger J, Narr KL (2013). White matter microstructure in subjects with attention-deficit/hyperactivity disorder and their siblings. *Journal of the American Academy of Child and Adolescent Psychiatry* **52**, 431–440, e434.

Lebel C, Warner T, Colby J, Soderberg L, Roussotte F, Behnke M, Davis Eyler F, Sowell ER (2013). White matter microstructure abnormalities and executive function in adolescents with prenatal cocaine exposure. *Psychiatry Research* **213**, 161–168.

Lin CP, Wedeen VJ, Chen JH, Yao C, Tseng WY (2003). Validation of diffusion spectrum magnetic resonance imaging with manganese-enhanced rat optic tracts and *ex vivo* phantoms. *Neuroimage* **19**, 482–495.

Lin HY, Gau SS, Huang-Gu SL, Shang CY, Wu YH, Tseng WY (2014). Neural substrates of behavioral variability in attention deficit hyperactivity disorder: based on ex-Gaussian reaction time distribution and diffusion spectrum imaging tractography. *Psychological Medicine* **44**, 1751–1764.

Liston C, Malter Cohen M, Teslovich T, Levenson D, Casey BJ (2011). Atypical prefrontal connectivity in attention-deficit/hyperactivity disorder: pathway to disease or pathological end point? *Biological Psychiatry* **69**, 1168–1177.

Lo YC, Soong WT, Gau SS, Wu YY, Lai MC, Yeh FC, Chiang WY, Kuo LW, Jaw FS, Tseng WY (2011). The loss of asymmetry and reduced interhemispheric connectivity in adolescents with autism: a study using diffusion spectrum imaging tractography. *Psychiatry Research* **192**, 60–66.

Luciana M, Nelson CA (1998). The functional emergence of prefrontally-guided working memory systems in four- to eight-year-old children. *Neuropsychologia* **36**, 273–293.

Makris N, Buka SL, Biederman J, Papadimitriou GM, Hodge SM, Valera EM, Brown AB, Bush G, Monuteaux MC, Caviness VS, Kennedy DN, Seidman LJ (2008). Attention and executive systems abnormalities in adults with childhood ADHD: a DT-MRI study of connections. *Cerebral Cortex* **18**, 1210–1220.

Martino J, De Witt Hamer PC, Berger MS, Lawton MT, Arnold CM, de Lucas EM, Duffau H (2013). Analysis of the subcomponents and cortical terminations of the perisylvian superior longitudinal fasciculus: a fiber dissection and DTI tractography study. *Brain Structure and Function* **218**, 105–121.

Mostofsky SH, Cooper KL, Kates WR, Denckla MB, Kaufmann WE (2002). Smaller prefrontal and premotor volumes in boys with attention-deficit/hyperactivity disorder. *Biological Psychiatry* **52**, 785–794.

Ni HC, Lin YJ, Gau SS, Huang HC, Yang LK (2013). An open-label, randomized trial of methylphenidate and atomoxetine treatment in adults with ADHD. *Journal of Attention Disorders* **16**, 1959–1973.

Pavuluri MN, Yang S, Kamineni K, Passarotti AM, Srinivasan G, Harral EM, Sweeney JA, Zhou XJ (2009). Diffusion tensor imaging study of white matter fiber tracts in pediatric bipolar disorder and attention-deficit/hyperactivity disorder. *Biological Psychiatry* **65**, 586–593.

Peters BD, Ikuta T, Derosse P, John M, Burdick KE, Gruner P, Prendergast DM, Szeszko PR, Malhotra AK (2014). Age-related differences in white matter tract microstructure are associated with cognitive performance from childhood to adulthood. *Biological Psychiatry* **75**, 248–256.

Peters BD, Szeszko PR, Radua J, Ikuta T, Gruner P, DeRosse P, Zhang JP, Giorgio A, Qiu D, Tapert SF, Brauer J, Asato MR, Khong PL, James AC, Gallego JA, Malhotra AK (2012). White matter development in adolescence: diffusion tensor imaging and meta-analytic results. *Schizophrenia Bulletin* **38**, 1308–1317.

Peterson DJ, Ryan M, Rimrodt SL, Cutting LE, Denckla MB, Kaufmann WE, Mahone EM (2011). Increased regional fractional anisotropy in highly screened attention-deficit hyperactivity disorder (ADHD). *Journal of Child Neurology* **26**, 1296–1302.

Reese TG, Heid O, Weisskoff RM, Wedeen VJ (2003). Reduction of eddy-current-induced distortion in diffusion MRI using a twice-refocused spin echo. *Magnetic Resonance in Medicine* **49**, 177–182.

Shang CY, Gau SS, Liu CM, Hwu HG (2011). Association between the dopamine transporter gene and the inattentive subtype of attention deficit hyperactivity disorder in Taiwan. *Progress in Neuro-Psychopharmacology and Biological Psychiatry* **35**, 421–428.

Shang CY, Wu YH, Gau SS, Tseng WY (2013). Disturbed microstructural integrity of the frontostriatal fiber pathways and executive dysfunction in children with attention deficit hyperactivity disorder. *Psychological Medicine* **43**, 1093–1107.

Silk TJ, Vance A, Rinehart N, Bradshaw JL, Cunnington R (2009). White-matter abnormalities in attention deficit hyperactivity disorder: a diffusion tensor imaging study. *Human Brain Mapping* **30**, 2757–2765.

Takahashi M, Iwamoto K, Fukatsu H, Naganawa S, Iidaka T, Ozaki N (2010). White matter microstructure of the cingulum and cerebellar peduncle is related to sustained attention and working memory: a diffusion tensor imaging study. *Neuroscience Letters* **477**, 72–76.

Tamm L, Barnea-Goraly N, Reiss AL (2012). Diffusion tensor imaging reveals white matter abnormalities in attention-deficit/hyperactivity disorder. *Psychiatry Research* **202**, 150–154.

Tseng WL, Gau SS (2013). Executive function as a mediator in the link between attention-deficit/hyperactivity disorder and social problems. *Journal of Child Psychology and Psychiatry* **54**, 996–1004.

Tuch DS (2004). Q-ball imaging. *Magnetic Resonance in Medicine* **52**, 1358–1372.

Tzourio-Mazoyer N, Landeau B, Papathanassiou D, Crivello F, Etard O, Delcroix N, Mazoyer B, Joliot M (2002). Automated anatomical labeling of activations in SPM using a macroscopic anatomical parcellation of the MNI MRI single-subject brain. *Neuroimage* **15**, 273–289.

van Ewijk H, Heslenfeld DJ, Zwiers MP, Buitelaar JK, Oosterlaan J (2012). Diffusion tensor imaging in attention deficit/hyperactivity disorder: a systematic review and meta-analysis. *Neuroscience and Biobehavioral Reviews* **36**, 1093–1106.

Veazie PJ (2006). When to combine hypotheses and adjust for multiple tests. *Health Services Research* **41**, 804–818.

Vestergaard M, Madsen KS, Baare WF, Skimminge A, Ejersbo LR, Ramsoy TZ, Gerlach C, Akeson P, Paulson

OB, Jernigan TL (2011). White matter microstructure in superior longitudinal fasciculus associated with spatial working memory performance in children. *Journal of Cognitive Neuroscience* **23**, 2135–2146.

Wakana S, Nagae-Poetscher LM, Jiang H, van Zijl P, Golay X, Mori S (2005). Macroscopic orientation component analysis of brain white matter and thalamus based on diffusion tensor imaging. *Magnetic Resonance in Medicine* **53**, 649–657.

Wedeen VJ, Wang RP, Schmahmann JD, Benner T, Tseng WY, Dai G, Pandya DN, Hagmann P, D'Arceuil H, de Crespigny AJ (2008). Diffusion spectrum magnetic resonance imaging (DSI) tractography of crossing fibers. *Neuroimage* **41**, 1267–1277.

Wu YH, Gau SS, Lo YC, Tseng WY (2014). White matter tract integrity of frontostriatal circuit in attention deficit hyperactivity disorder: association with attention performance and symptoms. *Human Brain Mapping* **35**, 199–212.

Yang HN, Tai YM, Yang LK, Gau SS (2013). Prediction of childhood ADHD symptoms to quality of life in young adults: adult ADHD and anxiety/depression as mediators. *Research in Developmental Disabilities* **34**, 3168–3181.

Yeh FC, Verstynen TD, Wang Y, Fernandez-Miranda JC, Tseng WY (2013). Deterministic diffusion fiber tracking improved by quantitative anisotropy. *PLoS ONE* **8**, e80713.

Yeh FC, Wedeen VJ, Tseng WY (2011). Estimation of fiber orientation and spin density distribution by diffusion deconvolution. *Neuroimage* **55**, 1054–1062.